2-2014

The Interaction of Photoactivators with Proteins during Microfabrication

Joseph W. Lafferty
Susquehanna University

James R. Strande
Susquehanna University

Peter M. Kerns
Susquehanna University

Nathan A. Fox
Susquehanna University

Swarna Basu
Susquehanna University

Recommended Citation

Joseph W. Lafferty, James R. Strande, Peter M. Kerns, Nathan A. Fox, Swarna Basu, The interaction of photoactivators with proteins during microfabrication, Journal of Photochemistry and Photobiology A: Chemistry, Volume 275, 1 February 2014, Pages 81-88, ISSN 1010-6030, http://dx.doi.org/10.1016/j.jphotochem.2013.10.017.

The Interaction of Photoactivators with Proteins during Microfabrication

Joseph W. Lafferty, James R. Strande, Peter M. Kerns, Nathan A. Fox and Swarna Basu*

Department of Chemistry, Susquehanna University, 514 University Avenue Selinsgrove, PA 17870

* Corresponding author. E-mail address: basu@susqu.edu; Tel.: 1-570-372-4223; fax: 1-570-372-2751

Abstract

Micron-scale protein cross-linking or microfabrication has been carried out using an Nd^{3+}-YAG laser as the excitation source. Fabrication is carried out by the excitation of photoactivators (Rose Bengal, methylene blue and 9-fluorenone-2-carboxylic acid) with the ultimate goal of creating stable structures that will serve as models for various applications (drug delivery and tissue engineering). Experimental parameters have been adjusted to minimize photodamage and maximize cross-linking efficiency. The higher than ideal photon flux and peak power necessitates the use of high protein concentrations to minimize photodamage. Rose Bengal and methylene blue are binding to proteins with high association constants ($K_a \approx 10^6$ M^{-1}) and both Rose Bengal and both 9-fluorenone-2-carboxylic acid are showing changes to their excited states

in presence of proteins at cross-linking concentrations. Molecular docking studies show that Rose Bengal binds close to the tryptophan with ΔG = -6.15 kcal/mol.

1. Introduction

Photopolymerization, also referred to as cross-linking or microfabrication or nanofabrication, is a process by which protein monomers are cross-linked via the excitation of a photoactivator or photosensitizer to form stable, bioactive structures [1-10]. New covalent bonds form between amino acid residues (tryptophan, tyrosine, cysteine, lysine, histidine) in adjacent proteins, without the loss of protein functionality [1-3]. Commonly-used photoactivators include Rose Bengal (RB), methylene blue (MB) or 9F2C (9-fluorenone-2-carboxylic acid) [1, 2, 6, 7]. Excitation can either be via a one-photon process or a multiphoton process. Multiphoton excitation (MPE) results in an intrinsic three-dimensional structure, as opposed to the two-dimensional structure that linear (one-photon) excitation provides [7, 8]. MPE photochemistry also provides a focal volume in which a high peak-power laser is tightly focused to produce fabrications on the micron-scale [7, 8, 10].

A Ti^{3+}: sapphire laser is typically used to cross-link proteins via multiphoton excitation of the photoactivator. In recent years, lower-cost systems have been developed and our group uses a setup that has a Nd^{3+}:YAG laser with a lower repetition rate and longer pulse width than most lasers used in this field [9]. The downside of using a low-cost system is the increase in power density at the focal point on the microscope slide. This results in the need for careful control of laser power and relative concentrations of proteins and photoactivators.

Aromatic amino acids, particularly tryptophan, are involved in photopolymerization. The singlet oxygen generated in the long-lived triplet state of RB induces a reaction with an aromatic amino acid such as tryptophan, leading to cross-linking [2]. The two most commonly studied proteins are the serum albumins, BSA (bovine) and HSA (human), due to their similar size and structure. The key difference between the two serum albumins is the number of Trp residues. BSA has two while HSA has only one. The only Trp residue within HSA (Trp 214) resides within a similar chemical environment to that of Trp 213 in BSA [11]. Lysozyme and fibrinogen have also been used for various cross-linking and protein/ligand interaction studies. Lysozyme contains a single amino acid chain and six Trp-residues, all of which are contained in the hydrophobic fold [12]. Fibrinogen and BSA fabrication efficiencies have been shown to be dependent on RB concentration. The two- to ten-fold fabrication rate increase of fibrinogen compared to BSA is due to its much larger molecular weight, 340 kg/mol, compare to 66 kg/mol for BSA. Naturally, this would result in a much larger volume of protein and many more potentially oxidizable residues. BSA provides fewer potential cross-linking sites and, therefore, is a suitable monomer to study the various mechanisms of photopolymerization with different photoactivators.

The xanthene compound Rose Bengal is a commonly-used photoactivator because of its efficiency in producing singlet oxygen in an aerobic environment [2]. Like RB, methylene blue is also a visible-absorbing photoactivator that has been used to cross-link proteins via a singlet oxygen mechanism [10, 13]. 9-fluorenone-2-carboxylic acid has seen limited use as a photoactivator but it has been used to cross-link a synthetic monomer via a three-photon process where hydrogen-abstraction is the mechanism [6]. The structures of the three photoactivators used in this work are shown in Fig. 1.

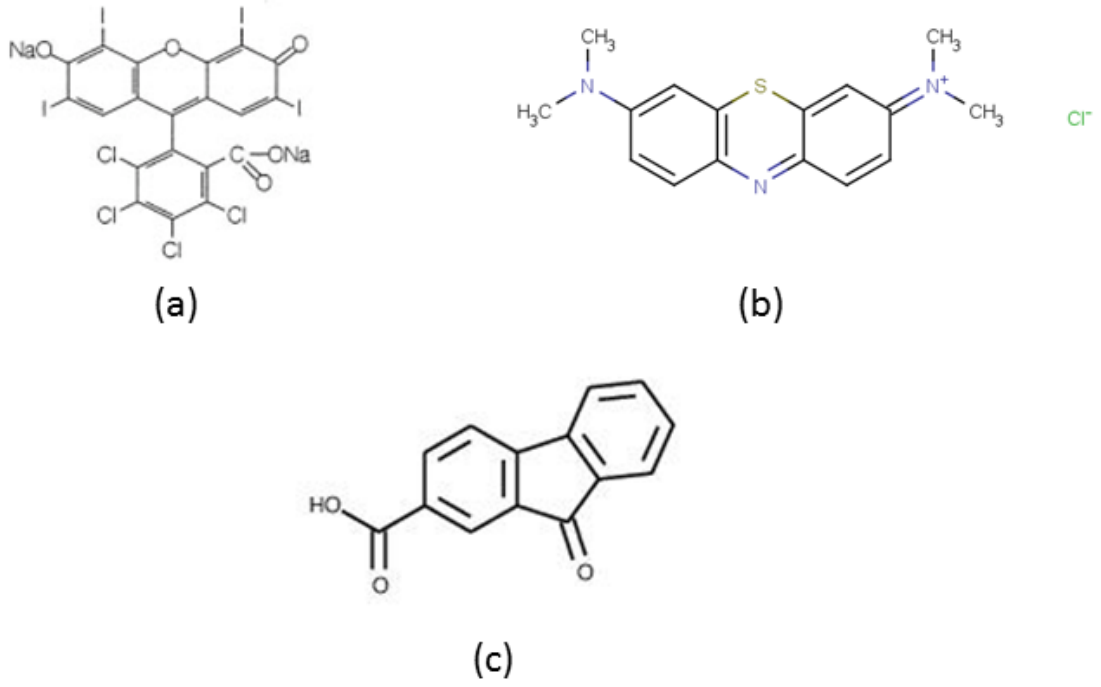

Fig. 1. The structures of the photoactivators used in this work. (a) Rose Bengal, (b) methylene blue, (c) 9-fluorenone-2-carboxylic acid.

In this work, a series of proteins have been successfully cross-linked using three photoactivators and a setup that offers higher than ideal peak power with an increased risk of photodamage. Since exposure dosage is a function of laser power per pulse, frequency and exposure time, these were all varied at specified concentration ratios of protein to photoactivator to determine optimum parameters for successful cross-linking. The relationship between the protein and photoactivator has also been investigated in an attempt to understand the exact nature of the physical interaction or proximity between the two species, and whether these interactions or proximity were a prerequisite for the formation of stable cross-linked structures.

2. Materials and Methods

2.1. Fabrication setup

The experimental setup has been described previously so only the modifications are reported here [9]. The current schematic is shown in Fig. 2. Briefly, the second harmonic (532nm, 5.9 ns pulse width) output of a Continuum Minilite II Nd^{3+}: YAG laser was directed into the Zeiss AxioObserver A1 inverted microscope laser port via one mirror (M1). The pulse is focused on the sample through the objective (Zeiss DC-Neofluar 20x, 0.5NA). Previously, three mirrors were used to direct the laser into the microscope port due to the height difference (0.9 mm) between the laser and the microscope's laser port. Due to a 70% loss of power from the laser source to the sample, the setup was modified to use only one mirror to direct the pulse from the source to the laser port of the microscope, leading to a 27% loss of power. Laser energy for optimal fabrication was 19.3 mJ per pulse, corresponding to a peak power of 3 MW. Images of fabricated structures were obtained using a ThorLabs DC310-C CCD camera.

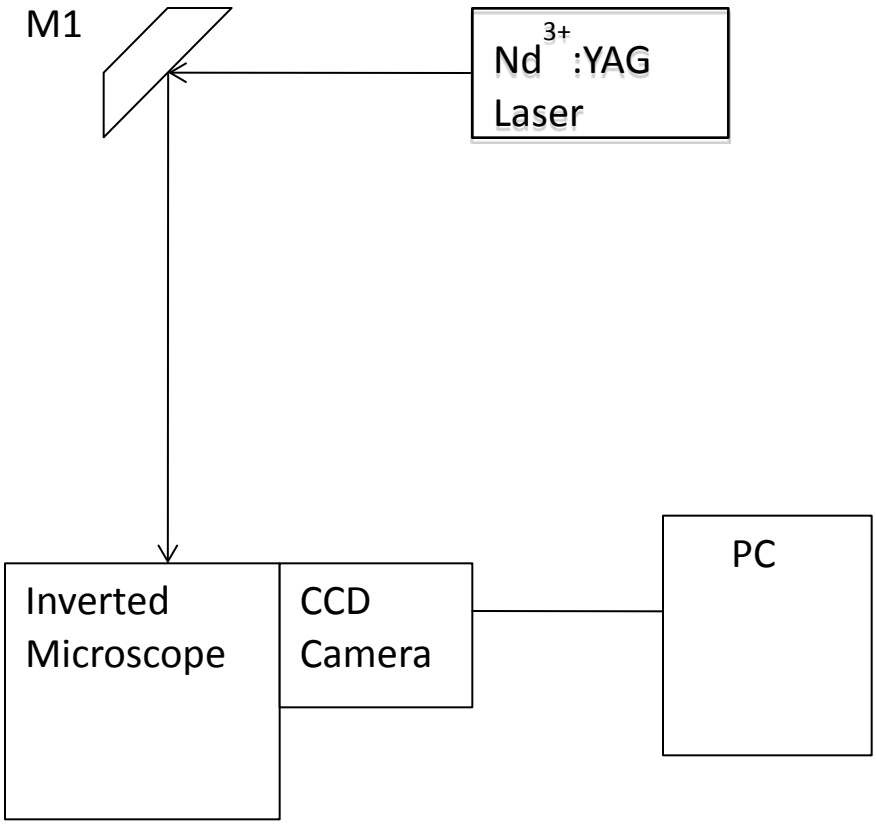

Fig. 2. Current schematic used for fabrication.

2.2. Chemicals and Fabrication Protocol

The photoactivators Rose Bengal (RB), methylene blue (MB) and 9-fluorenone-2-carboxylic acid (9F2C), and the proteins BSA, HSA, lysozyme and fibrinogen were obtained from Sigma-Aldrich and used without further purification. Protein stock solutions (100 mg/mL) were prepared in 50 mM tris buffer (pH = 7.0). RB and MB stock solutions were prepared in water and 9F2C stock solution was prepared in DMSO. Concentrations were verified using a Cary-Win 4000 UV-vis spectrometer.

Fabrication samples were prepared by adding the photoactivator stock directly to the protein solution in order to obtain concentration ratios that ranged from 40:1 (protein: photoactivator) to

1:4. For example, a 20:1 sample was prepared by adding 15 µL of the photoactivator (0.5 mM) to 100 µL of protein. The concentration of the stock solution of the photoactivator was adjusted to ensure that the maximum volume of photoactivator added was 15 µL. The small volume of DMSO added when using 9F2C did not affect the protein and this verified by comparing the protein's absorption and emission spectra in a buffer/DMSO mixture to a solution in buffer only. The emission spectra are shown in Fig. 3.

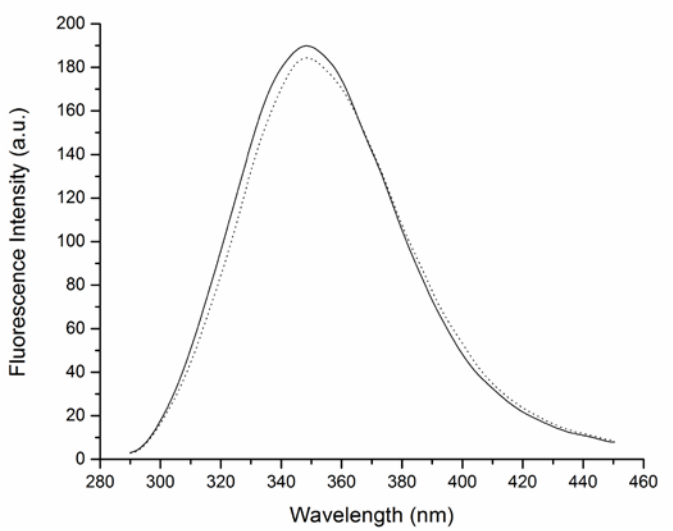

Fig. 3. Emission spectra of BSA in 100% tris buffer (solid line) and 13% DMSO/87% tris (dotted line) showing no changes to the protein's excited state or any evidence of denaturation. λ_{ex} = 280 nm. Excitation and emission slit widths were 3.0 nm.

The exposure dosage, time and frequency of the laser pulses were varied in order to determine optimal cross-linking parameters. Successful fabrication was achieved using pulse frequencies in the 8-15 Hz range with exposure times ranging from 7-15 seconds, with 10 Hz, 10 seconds being optimal for consistent fabrication. Fabrication was carried out on microscope slides that were treated according to a method described in the literature [14]. This was done to help the protein

cross-links adhere to the surface. However, protein cross-links also reliably adhered to untreated slides.

2.3. Fluorescence Quenching

For fluorescence quenching experiments, the protein concentration was fixed while the amount of quencher (RB, MB or 9F2C) was varied in each sample using a previously published protocol [11, 15]. All experiments were performed at room temperature using a Perkin-Elmer LS-50B Luminescence Spectrometer. Samples were excited at 280 nm and slit widths were set to 3 nm. Fluorescence spectra were then corrected for wavelength dependent sensitivity [16].

The dynamic or collisional quenching was investigated using the Stern-Volmer equation [11, 15, 17]

$$F_0/F = 1 + K_{SV}[Q] \quad (1)$$

F_0 and F correspond to the fluorescence intensities of the protein at 345 nm, without quencher and with quencher, respectively. $[Q]$ is the concentration of the quencher and K_{SV} is the Stern-Volmer quenching constant. K_{SV} is related to the lifetime of the system according to the following equation:

$$K_{SV} = k_q \tau_0 \quad (2)$$

k_q is the bimolecular quenching constant and τ_0 is the lifetime of unquenched tryptophan, which is typically 2.7 ns but longer (up to 9.8 ns) in proteins [18-20].

The static quenching or binding constant, K_a, and number of binding sites (n) between the protein and photoactivator were calculated using the following equation:

$$log\ [(F_0 - F)/F] = logK_a + nlog[Q] \quad (3)$$

2.4. Photoactivator Docking

Rose Bengal was docked against BSA using Autodock 4.2 and Python Molecule Viewer [21-23]. The protein was imported from the Protein Databank (PDB ID: 3V03). One chain of the two identical chains of the imported structure was removed. Waters were also deleted. The grid resolution was set to 1.00 Å, the grid size was set 62.00 x 62.00 x 62.00 Å. The two tryptophan residues, Trp134 and Trp213, were set to flexible. A Lamarckian Genetic Algorithm was performed using Autodock 4.2. The initial random population of structures was set to 150, the maximum number of energy evaluations per generation was 250000, and the maximum number of generations was 27000. The Lamarckian GA was run 10 times. Each docking concluded with the Solis and Wels local search method.

3. Results and Discussion

3.1. Optimization of Parameters for Fabrication

Fabrications with various concentration ratios of BSA to Rose Bengal were first carried out to establish the minimum exposure dosage required for cross-linking and the optimal concentration ratio of protein to photoactivator. Due to a low repetition rate (7-15 Hz) and high energy per pulse of the Nd^{3+}: YAG, a careful balance of these two parameters was required in order to avoid both glass damage and photodamage. Photodamage of the protein can occur via multiphoton excitation by two 532 nm photons, which provides the energy equivalent of a single 266 nm

photon, resulting in the direct excitation of the aromatic amino acid residues. Two photon absorption is possible even at low repetition rates as the UV-curable Norland Optical Adhesive was fabricated using our system. Therefore, the protein/photoactivator ratio played a critical role in this work.

Table 1 shows a comparison of peak power per pulse used in previously-published experiments, showing the correlation between peak power and concentration ratio. A higher protein to photoactivator ratio was necessary in this work because the higher peak power at the sample increased the odds of photodamage of the protein and therefore more protein was required. A higher pulse energy correlates to an increase in photons per pulse and in this work, the number of photons per pulse is 6-8 orders in magnitude higher than that used by groups that were able to work with concentration ratios lower than 1:1 [1, 6, 10, 24]. Clearly, more flexibility is available when higher repetition rates and shorter pulses are available but any issues with high peak power and pulse energy have been successful addressed.

Table 1

Comparison of laser pulse energy used for fabrication and the concentrations or proteins and photoactivators.

Reference	Pulse Energy (J)	Ratio	Concentrations	
			BSA	Photoactivator
[1]	6.6×10^{-11}	0.15	10 mg/mL	1 mM RB
[24]	1.3×10^{-9}	0.9	300 mg/mL	5 mM FAD
[10]	3.9×10^{-7}	0.75	200 mg/mL	4 mM RB
[6]	1.6×10^{-5}	0.15	10 mg/mL	1 mM RB
[25]	1.0×10^{-5}	1.5	400 mg/mL	4 mM RB
This Work	1.7×10^{-4}	16.8	100 mg/mL	90 µM RB
[9]	2.4×10^{-3}	31.5	10 mg/mL	4.76 µM RB

Fig. 4 shows a series of successful fabrications carried out with the various proteins and three photoactivators. The appearance of these structures was evidence of cross-linking as they did not form in the absence of a photoactivator. Photodamage was occasionally evident and these typically appeared as black circles that dissipated or floated away. The high protein concentration allowed for enough undamaged protein to be available for cross-linking.

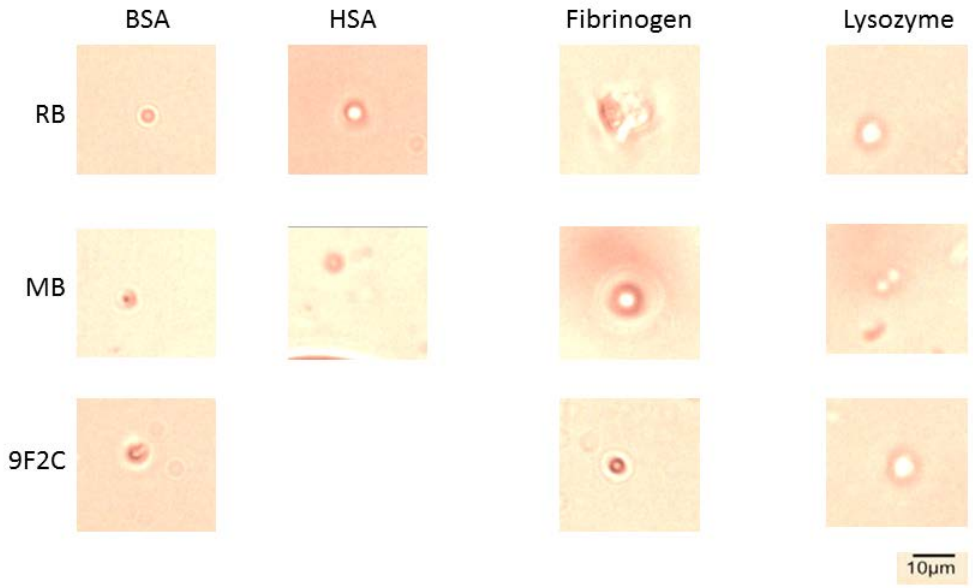

Fig. 4. Sample images of protein fabrications carried out with various photoactivators at a 20:1 concentration ratio. Exposure time was 10 seconds at a repetition rate of 10 Hz.

Fabrication was most successful when the concentration ratio ranged from 10:1 to 30:1, though some fabrication was observed at ratios as low as 1:4 but significant photodamage was visible and the structures were not stable and did not adhere to the slide.

Even at lower than usual photoactivator concentrations, the singlet oxygen generated by RB and MB was sufficient to promote cross-linking proteins in their proximity. The high protein concentration increased the odds of that occurring. Also, at 532 nm excitation, RB and MB were

accessing their S_1 state via direct one-photon excitation, rather than multiphoton excitation, which is the process used when Ti^{3+}:sapphire lasers (λ_{ex} = 740-800 nm) are used [2, 6, 10]. The theoretical feature size for the parameters (objective NA, excitation wavelength) based on the Abbe limit is 650 nm. However, one-photon excitation isn't restricted to the focal plane and out-of-plane excitation and photodamage is possible. The cross-linked structures ranged in size from 4-12 microns. The cross-linking efficiency was independent of the number of tryptophans in the protein as all combinations of protein and photoactivator required similar exposure doses at 20:1 concentration ratio to form stable cross-linked structures. Some photodamage is evident in the 9F2C cross-linked structures and the fabrications with fibrinogen are larger.

Of the four proteins studied, HSA was the only protein that had difficulty forming stable cross-links with 9F2C. Unlike RB and MB, 9F2C cannot be directly excited by a 532 nm pulse. It has an absorption maximum of 380 nm. As mentioned earlier, 9F2C has been used to cross-link a synthetic monomer via a three-photon process where three 780 nm photons offer the energy equivalent of a single 260 nm photon, which provides sufficient energy to excite the aromatic system [6]. In this work, two 532 nm photons will offer the same energy equivalence, making excitation of 9F2C possible. However, this will also directly excite the protein, increasing the likelihood of photodamage, which is evident in some of the fabrications (BSA/9F2C and fibrinogen/9F2C). HSA has only one tryptophan residue and this decreases the chances of successful fabrication as the tryptophan may be directly excited at the same time as 9F2C. Lysozyme has six tryptophan residues [12, 26] and cross-linking has been successfully achieved with 9F2C. The direct excitation of RB and MB by a 532 nm pulse along with their high absorption cross-sections lowers the chances of two-photon excitation of the protein.

3.2 Fluorescence Quenching

Fluorescence quenching experiments were carried out to determine the nature of the interaction between the proteins and the photoactivators. Quenching can either be static or dynamic in nature and can also be caused by FRET (fluorescence resonance energy transfer) [17, 27]. RB and MB cross-link via singlet-oxygen generation in their long-lived triplet states and 9F2C cross-links via hydrogen-abstraction. Whether or not these photoactivators have to be very close to the proteins, and whether they can cross-link at concentrations at high concentrations, is a question that has been addressed here.

All three photoactivators quenched the fluorescence of each protein when the concentration ratio of protein to photoactivator ranged from 6:1 to 1:1 (Fig. 5). The fluorescence quenching of BSA by RB and the corresponding static quenching plot is shown in Fig. 4. This shows that the photoactivator is forming a complex with the protein and that there is no long-range energy transfer from the protein to the photoactivator. RB absorbs at longer wavelength (549 nm) than the emission wavelength of tryptophan (345 nm). The absence of spectral overlap, in addition to the non-linear nature of the dynamic quenching plot (not shown), confirms that the quenching is static in nature, and not due to FRET (fluorescence resonance energy transfer) [11, 15, 17]. An important thing to note is that for dynamic quenching, the maximum value of k_q is normally in the range of 2.0×10^{10} $M^{-1}s^{-1}$ [11, 15, 28, 29]. The Stern-Volmer constants, K_{SV}, were on the order of 10^5. In the case of the proteins and free Trp, τ_0 is small (10^{-8} to 10^{-9} s) [27], and using Eqn. 2, this gives k_q values on the order of 10^{13}-10^{14}, much higher than those expected for dynamic quenching. Molecular Docking studies were carried out to confirm that the binding of photoactivators occurred in close proximity to the tryptophan residues.

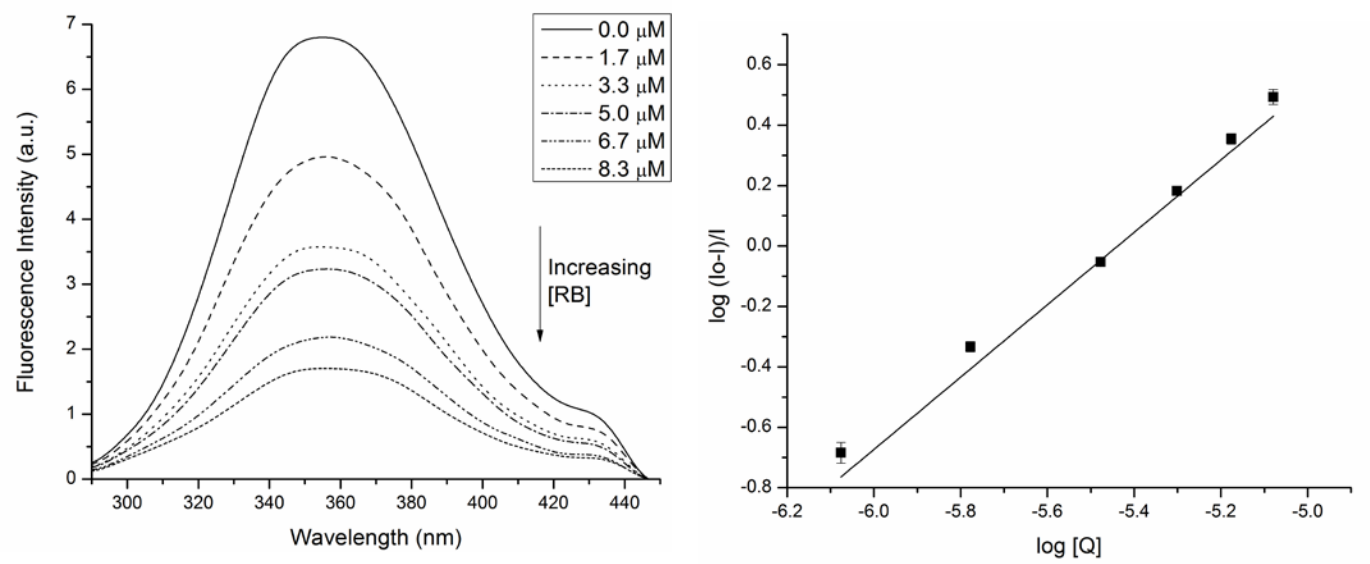

Fig. 5. (a) A typical fluorescence quenching plot showing the fluorescence spectra of BSA (1.0 x 10^{-5} M) in the presence of different concentrations of RB. λ_{ex} = 280 nm, λ_{em} = 345 nm. Excitation and emission slit widths were 3.0 nm. Fluorescence data was corrected for wavelength-dependent sensitivity and smoothed for presentation purposes. (b) Stern-Volmer plot for static quenching (R^2 = 0.9747) of BSA by RB. The association constant, K_a is on the order of 10^6 and the binding site number, *n*, is 1.

Table 2 shows a summary of all binding constants, K_A, and binding site numbers, *n*, for some of the protein-photoactivator systems. In a majority of cases, the photoactivator is binding favorably to one site in the protein and the association is thermodynamically favorable ($K_A > 10^5$; $\Delta G << 0$). The exclusion of 9F2C will be described shortly.

Table 2. Summary of binding constant, K_a, and binding site number, n, for the different protein-photoactivator systems.

Photoactivator	**BSA**		**HSA**		**Fibrinogen**		**Lysozyme**	
	K_a, M^{-1}	n	K_a, M^{-1}	n	K_a, M^{-1}	n	K_a, M^{-1}	n
Rose Bengal	2.2×10^6	1	3.2×10^6	1	3.2×10^5	1	1.3×10^6	1
Methylene Blue	7.8×10^6	1	2.7×10^6	1	3.8×10^6	1	7.5×10^6	1

Fabrication was most successful when the concentration ratio ranged from 10:1 to 30:1, with 20:1 being optimal. At higher photoactivator concentrations, fabrication occurred only when the repetition rate was increased and even then the probability of successful fabrication was diminished. As illustrated in Fig. 5 (a), fluorescence quenching of BSA is significant at micromolar concentrations of photoactivator. 1.7 µM corresponds to a concentration ratio of 6:1, where fabrication was occurring but the structures were either not stable or sustained photodamage (Fig. 6).

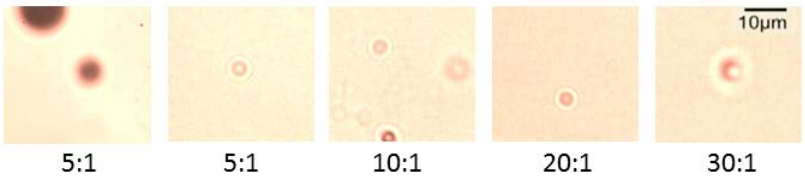

Fig. 6. Images of BSA/RB fabrication over a wide range of concentration ratios, with evidence of successful cross-linking and photodamage at 5:1. Some photodamage is also evident at 10:1.

At the higher protein concentrations (ratio of 10:1 and greater), fluorescence quenching was negligible. Therefore, at higher RB concentrations, the photoactivator is binding to the protein with a high binding constant and this either appears to affect its ability to generate singlet oxygen and promote cross-linking or the binding inhibits access to the tryptophan and the singlet oxygen

cannot target the tryptophan. In order to test the second possibility, a nickel complex known to strongly bind to proteins [11] was added to the protein solution at the same ratio where significant fluorescence quenching was occurring. RB was then added so that the protein/RB ratio was 20:1 and no cross-linking occurred, even when the exposure dose was adjusted. Therefore, the presence of a static quencher at high concentrations leads to the binding of the quencher near the tryptophan, blocking access to it and inhibiting cross-linking. A third possibility is that while two-photon excitation of the protein may occur at any time, the lower protein concentration (10:1 and lower) increases the odds of photodamage as there is a smaller amount of protein in the focal volume. Therefore, the ability to consistently and reliably cross-link at 20:1 is due to a combination of factors: photoactivators that are not bound to the protein (but are likely to be close enough to transfer singlet oxygen) and the high concentration of protein that can withstand the excess energy and possible two-photon excitation.

Fluorescence quenching is often a result of energy transfer from a donor (tryptophan) to an acceptor (photoactivator) [30]. Excluding 9F2C, in all the systems and combinations studied, the quenching of tryptophan fluorescence is static and Forster's long-range energy transfer is not taking place in the case of RB and MB. As mentioned earlier, the spectral overlap between tryptophan emission band and absorption bands for RB and MB is negligible compared to other systems [31, 32]. The presence of an overlap between the emission band of the donor and the absorption band of the acceptor is a requirement for FRET [15, 33]. Therefore, both RB and MB are quenching the fluorescence *via* a thermodynamically favorable ($\Delta G < 0$) interaction with a high binding constant. For 9F2C, both the dynamic and static quenching plots deviate from linearity at high 9F2C concentrations. The non-linear nature of the dynamic quenching plot is

indicative of static quenching and that is observed with RB and MB. But the non-linear nature of the static quenching plots raises further questions about the interaction between 9F2C and the proteins.

Unlike RB and MB, the absorption band of 9F2C overlaps with the emission band of the protein (Fig. 7), but the extinction coefficient of 9F2C is very low (411 L mol^{-1} cm^{-1} at 380 nm). The spectral overlap is 7.0255 x 10^{-16} cm^3 L mol^{-1} and the Forster distance, R_0, is 1.51 nm, which is lower than the 2-6 nm range over which FRET occurs [33].

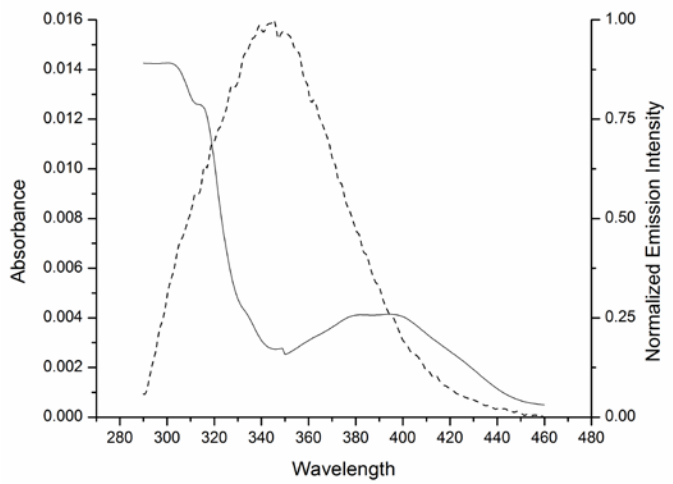

Fig. 7. Emission spectrum of HSA (1.0 x 10^{-5} M) and the calculated absorption spectrum of 9F2C (1.0 x 10^{-5} M). The absorption spectrum was calculated using extinction coefficients obtained from the absorption spectrum of 0.5 mM 9F2C.

Even though the spectral overlap makes 9F2C an ideal candidate for energy transfer from proteins, its low extinction coefficient lowers the probability. At the same time, it is difficult to ascertain whether or not it is binding to proteins at or below cross-linking concentrations. While

stable cross-links were formed with BSA, fibrinogen and lysozyme, HSA was difficult to cross-link with 9F2C. The protein concentrations required for this work was 100 mg/mL and this is tenfold higher than the solubility limit for lysozyme. The high concentration was achievable for short periods of time and the fabrication samples for BSA, HSA and fibrinogen showed no evidence of precipitation, but the presence of a small amount of DMSO (15 µL in a 115 µL fabrication sample) was did affect the solubility of lysozyme, therefore the cross-linking window was very narrow. When cross-links did form, they were not always stable and did not readily adhere to the slide. But success with cross-linking in a solvent system that is not 100% aqueous opens up the possibility for the design of photoactivators that are not water-soluble but still function at physiological pH.

3.3 Effect of Protein on Photoactivator Excited State

In the previous section we have detailed the nature of the interaction between the protein and the photoactivator. This raises the question about the photoactivator itself. What changes, if any, might be taking place to the photoactivator? In order to determine this, the emission spectrum of each photoactivator was measured in the presence and absence of BSA, at the same concentration ratio (20:1) that was most ideal for fabrication. Of the three photoactivators, 9F2C and RB showed small changes to its excited state and the change was independent of the concentration ratio.

Fig. 8 shows the emission spectra of the various photoactivators with and without BSA. In the presence of the protein, the emission peak of RB red-shifts by approximately 18 nm and the

emission peak of 9F2C red-shifts by approximately 15 nm. The emission peak of MB does not shift.

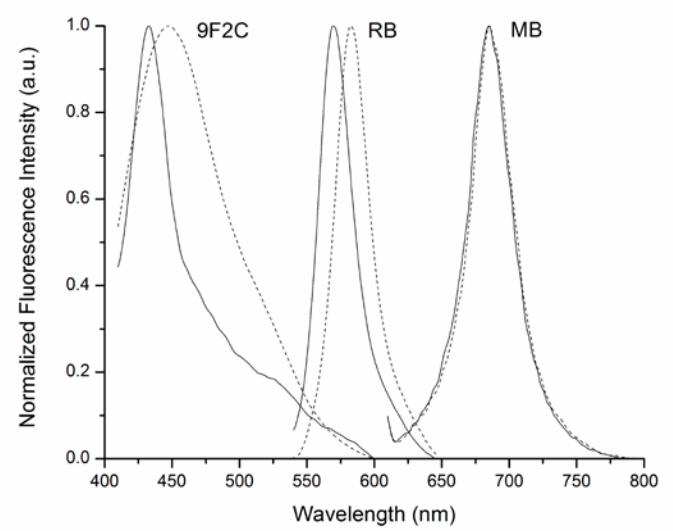

Fig. 8. Emission spectra of the photoactivators, without (solid line) and with BSA (dashed line). The excitation wavelength is 532 nm for RB and MB, corresponding to the second harmonic of the Nd^{3+}:YAG laser, and 380 nm for 9F2C. Fabrication samples were diluted 100-fold in order to eliminate concentration quenching and detector saturation.

In the case of RB, a smaller (5 nm) red-shift was reported in the presence of hyper-branched polyglycols and was attributed to a change in the dye's microenvironment as a result of a tighter complexation with its counterion [34]. RB is an anionic dye [35] and in this work, the sodium salt of Rose Bengal was used and the red-shift can be attributed to the complexation of RB with BSA in presence of its counterion. The complexation of Rose Bengal with proteins has also been reported in the literature [36]. In that study, the protein (BSA) was used as the quencher and the RB concentration was significantly higher than that of the protein, unlike this work. The red-shift of the RB emission peak has also been attributed to the formation of aggregates in solution [35]

but when those aggregates form, the free (monomer) RB shows a blue-shift in the excitation spectrum which is not occurring here. The corresponding excitation spectrum of RB is unchanged.

No change is observed in the excitation and emission spectra of MB, which is a cationic dye but 9F2C displayed a 25 nm blue-shift in its excitation spectrum upon addition of BSA along with a 15 nm red-shift in its emission spectrum. 9F2C is a neutral molecule capable of both H-bonding and pi-stacking due to its extended pi-system. Stronger H-bonding results in a blue-shift of absorption bands. Since 9F2C has multiple H-bonding locations and can undergo n $\rightarrow \pi^*$ transitions, the lone pair is stabilized in the ground state due to H-bonding, resulting in a lowering of energy of the orbital and an increase in the energy gap. Also, in addition to binding tightly to proteins at lower protein/photoactivator ratios, aggregation in a H-type (layered) form is also possible as that would be most energetically favorable given that pi-stacking can occur [35].

3.4 Photoactivator Docking

Molecular docking studies were carried out to determine if the photoactivators were docking at or near the tryptophan residue in proteins and if they were docking, whether or not the interaction was favorable.

Of the ten dockings that were carried out for BSA/RB, RB docked adjacent to tryptophan in three dockings. Besides the energetic preference, the calculated inhibition constant of the tryptophan-adjacent dockings tended to be much lower than that of energetically close dockings. The most energetically favored docking was adjacent to tryptophan 213 (2.971 Å, Fig. 9) with a

binding energy of -6.15 kcal/mol. This compares favorably with the K_A value for BSA-RB reported in Table 2. The K_A of 2.2 x 10^6 M^{-1} corresponds to a ΔG value of -8.6 kcal/mol. RB prefers to interact with the protein via hydrophobic interactions. The amino acids adjacent to Trp 213 are hydrophobic and neutral, while the amino acids adjacent to Trp 134 are either hydrophobic or charged. In two other dockings (not shown), Rose Bengal docked adjacent to tryptophan 134 (4.119 Å and 6.994 Å, respectively) and the binding energies were -5.23 kcal/mol and -2.81 kcal/mol, respectively.

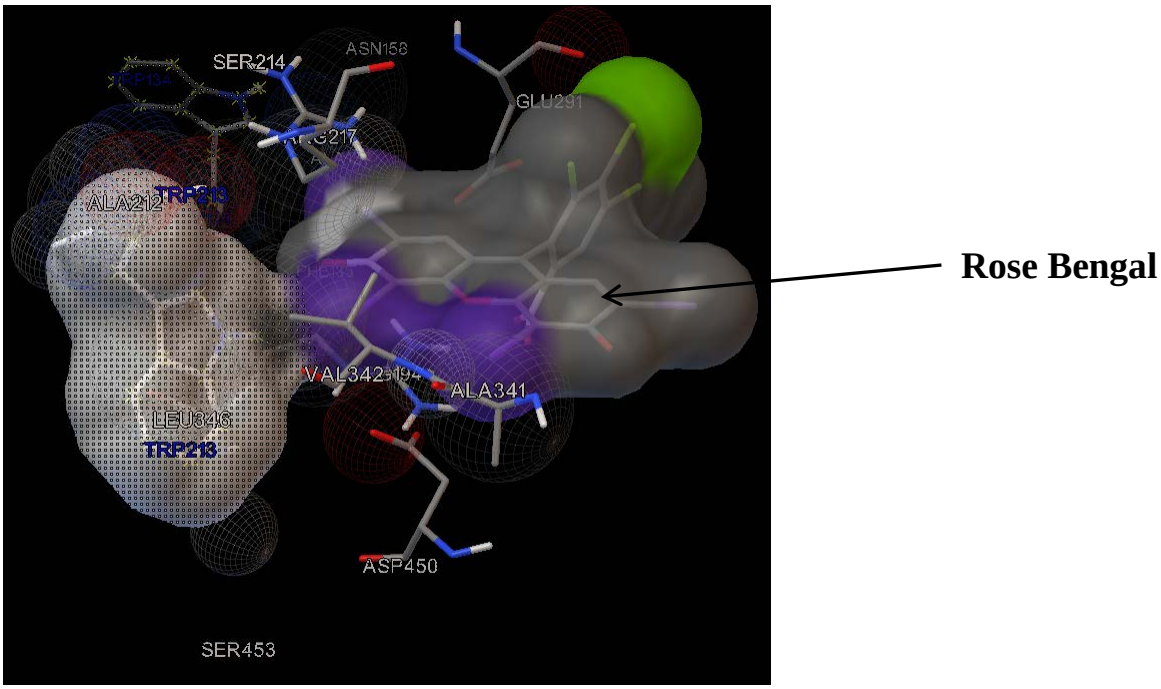

Fig. 9. Tryptophan-213 and adjacent residues interacting with the Rose Bengal in the most energetically favored docking (Binding energy = -6.15 kcal/mol). The spheres indicate hydrogen bonding, Rose Bengal's surface is colored for electronegativity, the merging of surfaces indicates that Rose-Bengal is energetically favored interacting electronically with tryptophan. Red spheres indicate a breaching of the Van der Waals atomic radius beyond the well depth. White spheres are indicative of breaching that is less than at the VdW well depth.

4. Conclusion

Protein cross-linking has been successfully carried out using a Nd^{3+}:YAG laser. Three different photoactivators have been used and the cross-linking parameters have been optimized to minimize photodamage and maximize cross-linking efficiency. Parameters have been compared to other published studies and a correlation has been observed between peak pulse power and protein concentration. Two of the three photoactivators have been shown to tightly bind to the proteins and statically quench the fluorescence of the tryptophan. The quenching occurs at photoactivator concentrations higher than what was suitable for cross-linking but it is clear that the photoactivator is involved in a short-range interaction with the protein prior to cross-linking. This binding has been confirmed by Autodock 4.2, which showed that Rose Bengal docked closest (2.971 Å) to Trp-213 in BSA. The excited states of Rose Bengal and 9F2C are also showing changes in presence of the protein.

Acknowledgements

The authors thank Susquehanna University for its financial support and the George I. Alden Trust for providing the funding for the pulsed laser and inverted microscope. The authors also thank the II-VI Foundation for its support for undergraduate research.

References

[1] S. Basu, P.J. Campagnola, J Biomed Mater Res A 71 (2004) 359-368.
[2] S. Basu, P.J. Campagnola, Biomacromolecules 5 (2004) 572-579.
[3] S. Basu, L.P. Cunningham, G.D. Pins, K.A. Bush, R. Taboada, A.R. Howell, J. Wang, P.J. Campagnola, Biomacromolecules 6 (2005) 1465-1474.
[4] S. Basu, V. Rodionov, M. Terasaki, P.J. Campagnola, Opt Lett 30 (2005) 159-161.
[5] S. Basu, C.W. Wolgemuth, P.J. Campagnola, Biomacromolecules 5 (2004) 2347-2357.
[6] J.D. Pitts, P.J. Campagnola, G.A. Epling, S.L. Goodman, Macromolecules 33 (2000) 1514-1523.

[7] J.D. Pitts, A.R. Howell, R. Taboada, I. Banerjee, J. Wang, S.L. Goodman, P.J. Campagnola, Photochem Photobiol 76 (2002) 135-144.
[8] M. Sridhar, S. Basu, V.L. Scranton, P.J. Campagnola, Rev Sci Instrum 74 (2003) 3474-3477.
[9] G. Trout, S. Basu, Meas Sci Technol 20 (2009) 127001.
[10] B. Kaehr, N. Ertas, R. Nielson, R. Allen, R.T. Hill, M. Plenert, J.B. Shear, Anal Chem 78 (2006) 3198-3202.
[11] H.F. Crouse, J. Potoma, F. Nejrabi, D.L. Snyder, B.S. Chohan, S. Basu, Dalton Trans 41 (2012) 2720-2731.
[12] T. Imoto, L.S. Forster, J.A. Rupley, F. Tanaka, Proc Natl Acad Sci USA 69 (1972) 1151-1155.
[13] R. Allen, R. Nielson, D.D. Wise, J.B. Shear, Anal Chem 77 (2005) 5089-5095.
[14] P.-J. Su, Q.A. Tran, J.J. Fong, K.W. Eliceiri, B.M. Ogle, P.J. Campagnola, Biomacromolecules 13 (2012) 2917-2925.
[15] H.F. Crouse, E.M. Petrunak, A.M. Donovan, A.C. Merkle, B.L. Swartz, S. Basu, Spec Lett 44 (2011) 369-374.
[16] C.M. Schneck, A.J. Poncheri, J.T. Jennings, D.L. Snyder, J.L. Worlinsky, S. Basu, Spectrochim Acta A Mol Biomol Spectrosc 75 (2010) 624-628.
[17] J.R. Lakowicz, Principles of Fluorescence Spectroscopy, Springer Science, U.S.A., 2004.
[18] R. Swaminathan, G. Krishnamoorthy, N. Periasamy, Biophys J 67 (1994) 2013-2023.
[19] H.M. Rawel, S.K. Frey, K. Meidtner, J. Kroll, F.J. Schweigert, Mol Nutr Food Res 50 (2006) 705-713.
[20] C. Formoso, L.S. Forster, J Biol Chem 250 (1975) 3738-3745.
[21] G.M. Morris, R. Huey, W. Lindstrom, M.F. Sanner, R.K. Belew, D.S. Goodsell, A.J. Olson, J Comp Chem 30 (2009) 2785-2791.
[22] G.M. Morris, D.S. Goodsell, R.S. Halliday, R. Huey, W.E. Hart, R.K. Belew, A.J. Olson, J Comp Chem 19 (1998) 1639-1662.
[23] D.S. Goodsell, G.M. Morris, A.J. Olson, J Mol Recog 9 (1996) 1-5.
[24] R.T. Hill, J.B. Shear, Anal Chem 78 (2006) 7022-7026.
[25] S. Peltola, M. Kellomaki, J. Viitanen, Laser Inst America 101 (2008) 403/493-n403/498.
[26] T. Imoto, L.N. Johnson, A.T.C. North, D.C. Phillips, J.A. Rupley, Lysozyme in Enzymes, Academic Press, New York, 1972.
[27] M.R. Eftink, C.A. Ghiron, Anal Biochem 114 (1981) 199-227.
[28] S.H. Laurie, D.E. Pratt, J Inorg Biochem 28 (1986) 431-439.
[29] K.I. Sugae, B. Jirgensons, J Biochem 56 (1964) 457-464.
[30] H.Y. Shrivastava, B.U. Nair, J Inorg Biochem 98 (2004) 991-994.
[31] M.R. Eftink, C.A. Ghiron, Anal Biochem 114 (1981) 199-227.
[32] D. Wu, Q. Wei, Y. Li, B. Du, G. Xu, Int J Biol Macromol 37 (2005) 69-72.
[33] J.B. Xiao, J.W. Chen, H. Cao, F.L. Ren, Y. Yang, C.S. Chen, M. Xu, J Photochem Photobiol A: Chemistry 191 (2007) 222-227.
[34] E. Burakowska, J.R. Quinn, S.C. Zimmerman, R. Haag, J Am Chem Soc 131 (2009) 10574-10580.
[35] D. Xu, D.C. Neckers, J Photochem Photobiol A: Chemistry 40 (1987) 361-370.
[36] T. Perez-Ruiz, C. Martinez-Lozano, V. Tomas, J. Fenoll, Analyst 125 (2000) 507-510.